

# The interpolating formula for the $0\nu\beta\beta$ -decay half-life in the case of light and heavy neutrino mass mechanisms

A. Babič,<sup>1,2,3</sup> S. Kovalenko,<sup>4</sup> M.I. Krivoruchenko,<sup>3,5</sup> and F. Šimkovic<sup>6,7,8</sup>

<sup>1</sup>*Dept. of Dosimetry and Application of Ionizing Radiation,  
Czech Technical U., 115 19 Prague, Czech Rep.*

<sup>2</sup>*Institute of Experimental and Applied Physics,  
Czech Technical University, 128 00 Prague, Czech Republic*

<sup>3</sup>*Bogoliubov Laboratory of Theoretical Physics, Joint Institute for Nuclear Research, 141980 Dubna, Russia*

<sup>4</sup>*Universidad Técnica Federico Santa María, Centro-Científico-Tecnológico de Valparaíso, Casilla 110-V, Valparaíso, Chile*

<sup>5</sup>*Institute for Theoretical and Experimental Physics,  
B. Cheremushkinskaya 25, 117218 Moscow, Russia*

<sup>6</sup>*Department of Nuclear Physics and Biophysics, Comenius University,  
Mlynská dolina F1, SK-842 15 Bratislava, Slovakia*

<sup>7</sup>*Bogoliubov Laboratory of Theoretical Physics, JINR, 141980 Dubna, Moscow Region, Russia*

<sup>8</sup>*Czech Technical University in Prague, CZ-12800 Prague, Czech Republic*

We revisit the “interpolating formula” proposed in our previous publication. It allows one to calculate the  $0\nu\beta\beta$ -decay half-life for arbitrary neutrino mass without involvement of the complicated results for nuclear matrix elements (NME) obtained within specific nuclear structure models. The formula derives from the finding that the value of a properly normalized ratio of the NMEs for the light and heavy neutrino mass mechanisms weakly depends on isotope. From this fact it follows, in particular, that the light and heavy neutrino mass mechanisms can hardly be distinguished in a model independent way searching for  $0\nu\beta\beta$ -decay of different nuclei. Here we show that this formula holds for all the known nuclear structure approaches. We give a mathematical justification of our results examining analytical properties of the NMEs. We also consider several simplified benchmark scenarios within left-right symmetric models and analyze the conditions for the dominance of the light or heavy neutrino mass mechanisms in  $0\nu\beta\beta$ -decay.

## I. INTRODUCTION

Neutrinoless double beta ( $0\nu\beta\beta$ ) decay is a Lepton Number Violating (LNV) process changing lepton number in two units  $\Delta L = 2$ . It is forbidden in the Standard Model (SM), where lepton number is conserving. Basically there are two sources of LNV: Majorana neutrino mass and LNV vertices. The latter may emerge from numerous high-scale models giving rise to the corresponding mechanisms of  $0\nu\beta\beta$ -decay. Once this process is observed, the question of distinguishing between the dominant mechanisms will arise. Certainly, this task is highly non-trivial. One may hope that measurements of  $0\nu\beta\beta$  half-life with different isotopes would facilitate its solution due to variability of Nuclear Matrix Elements (NME) of particular mechanisms from one isotope to the other. In the present paper we show that at least the light and heavy Majorana neutrino mass mechanisms are indistinguishable in this way without additional hypothesis. This fact becomes especially comprehensible in terms of the so called “interpolating formula” (IntF)[8] merging the light and heavy neutrino mass ranges in the NMEs and allowing a transparent physical interpretation of the above fact. The IntF is a simple analytical formula representing with an accuracy of 30% or better the NME as a function of the Majorana neutrino mass. This accuracy is sufficient for practical purposes taking into account the limited accuracy of the available nuclear structure approaches to the NME calculations. In what follows we will show that that the IntF

is valid for all these nuclear structure approaches with the above-indicated accuracy and elucidate some of its other useful properties. On the particle physics side we adopt a generic scenario with Majorana neutrinos of arbitrary value masses and consider their contribution to  $0\nu\beta\beta$ -decay via mass mechanism mediated by both left- and right-handed weak currents. Then for the sake of concreteness we consider the neutrino mass mechanism within the left-right symmetric models (LRS) [3, 4] and extent our analysis towards some more particular scenarios.

## II. NEUTRINO MASS MECHANISM OF $0\nu\beta\beta$ -DECAY

We start with a generic Majorana neutrino mass mechanism of  $0\nu\beta\beta$ -decay induced by the low-energy effective Lagrangian

$$\mathcal{L}^\beta = \frac{G_\beta}{\sqrt{2}} \left[ j_L^\rho J_{L\rho}^\dagger + \lambda j_R^\rho J_{R\rho}^\dagger + h.c. \right] \quad (1)$$

with the left/right-handed hadronic  $J_{L/R}$  and leptonic  $j_{L/R}$  currents. As usual,  $G_\beta = G_F \cos \theta_C$ , where  $G_F$  and  $\theta_C$  are Fermi constant and Cabbibo angle, respectively. The dimensionless parameter  $\lambda$  depends on the underlying high-scale model. In the particular case of the Left Right Symmetric (LRS) models, based on the  $SU(2)_L \otimes SU(2)_R \otimes U(1)_{B-L}$  gauge group [3, 4], the Lagrangian (1) appears at low energies after integrating

out  $W_{L,R}^\pm$  massive gauge bosons. In this model

$$\lambda = (M_{W_L}/M_{W_R})^2, \quad (2)$$

where  $M_{W_L}$  and  $M_{W_R}$  ( $M_L < M_R$ ) are masses of  $W_L$  and  $W_R$  gauge bosons, respectively. The current constrain on the mass of  $W_R$  is  $M_{W_R} \geq 2.9$  TeV [15] sets the limit

$$\lambda \leq 7.7 \times 10^{-4}. \quad (3)$$

The upper limit  $\lambda = 7.7 \times 10^{-4}$  we use everywhere in the present paper as a reference value for this parameter. Since we focus on the mass mechanism we discarded in Eq. (1) the  $j_{L,R} J_{R,L}$  terms irrelevant in this case (for a review see, for instance [1]). In Eq. (1) the explicit form of the left- and right-handed hadronic currents  $J_{L,R}^\dagger$  in nuclei can be found, e.g., in Ref. [7]. The leptonic currents are given by

$$j_L^\rho = \bar{e}_L \gamma^\rho \nu'_{eL}, \quad j_R^\rho = \bar{e}_R \gamma^\rho \nu'_{eR}.$$

The  $\nu'_{eL}$  and  $\nu'_{eR}$  are the weak eigenstate electron neutrinos, which are expressed as superpositions of the light and heavy Majorana mass eigenstate neutrinos  $\nu_j$  and  $N_k$  as

$$\begin{aligned} \nu'_{eL} &= \sum_{j=1}^3 U_{ej} \nu_j + \sum_{k=1}^n S_{ek} N_k^C, \\ \nu'_{eR} &= \sum_{j=1}^3 T_{ej}^* \nu_j^C + \sum_{k=1}^n V_{ek}^* N_k, \end{aligned} \quad (4)$$

where the unitary matrix

$$\mathcal{U} = \begin{pmatrix} U & S \\ T & V \end{pmatrix}. \quad (5)$$

is the generalizations of the Pontecorvo-Maki-Nakagawa-Sakata (PMNS) matrix, which diagonalizes the general  $(3+n) \times (3+n)$  neutrino mass matrix

$$\mathcal{M} = \begin{pmatrix} M_L & M_D \\ M_D^T & M_R \end{pmatrix} \quad (6)$$

in the basis  $(\nu'_{eL}, \nu'_{\mu L}, \nu'_{\tau L}, N_{1R}^C, \dots, N_{nR}^C)$ . Here  $M_{L,R}$  and  $M_D$  are Majorana and Dirac mass terms, respectively. After diagonalization one should end up with 3 light  $\nu_i$  ( $i=1,2,3$ ) and  $n$  heavy  $N_k$  ( $k=1,\dots,n$ ) Majorana neutrino mass eigenstates with the masses  $m_i$  and  $M_k$ , respectively. In the LRS models  $n=3$ . The smallness of  $m_i$  can be guaranteed by the seesaw-I condition  $M_R \gg M_D$ . As is well known this leads to very heavy states  $N_k$  with masses  $M_k \gg 1$  TeV being beyond the experimental reach. In the scenarios with  $n > 3$  the inverse seesaw mechanism can be implemented. In this case among  $N_k$ , accompanying the light  $\nu_i$  states, there can appear moderately heavy or even light Majorana states. Actually, their masses can be of arbitrary value. This is the case of our particular interest, for which we designed the above-mentioned interpolating formula.

Assuming the dominance of the mass mechanism we write down the  $0\nu\beta\beta$ -decay half-life

$$\begin{aligned} [T_{1/2}^{0\nu}]^{-1} &= G^{0\nu} g_A^4 m_p^2 \times \\ &\left( \left| \sum_{j=1}^3 U_{ej}^2 m_j M_{LL}^{\prime 0\nu}(m_j) + \sum_{k=1}^n S_{ek}^2 M_k M_{LL}^{\prime 0\nu}(M_k) \right|^2 \right. \\ &\left. + \lambda^2 \times \right. \\ &\left. \left| \sum_{j=1}^3 T_{ej}^2 m_j M_{RR}^{\prime 0\nu}(m_j) + \sum_{k=1}^n V_{ek}^2 M_k M_{RR}^{\prime 0\nu}(M_k) \right|^2 \right). \end{aligned} \quad (7)$$

The proton mass is denoted by  $m_p$  and  $g_A$  is the unquenched value of axial-vector coupling constant ( $g_A = 1.269$ ). The phase-space factor  $G^{0\nu}$  is tabulated for various  $0\nu\beta\beta$ -decaying nuclei in Ref. [9]. The NMEs  $M^{\prime 0\nu}$  as functions of neutrino mass  $m_\nu$  ( $m_\nu = m_i$  or  $M_k$ ) are given by [8]

$$\begin{aligned} M_{LL,RR}^{\prime 0\nu}(m_\nu) &= \frac{1}{m_p m_e} \frac{R}{2\pi^2 g_A^2} \sum_n \int d^3x d^3y d^3p \\ &\times e^{i\mathbf{p}\cdot(\mathbf{x}-\mathbf{y})} \frac{\langle 0_F^+ | J_{L,R}^{\mu\dagger}(\mathbf{x}) | n \rangle \langle n | J_{L,R}^\dagger{}_\mu(\mathbf{y}) | 0_I^+ \rangle}{\sqrt{p^2 + m_\nu^2} (\sqrt{p^2 + m_\nu^2} + E_n - \frac{E_I - E_F}{2})}. \end{aligned} \quad (8)$$

Here,  $R$  and  $m_e$  are the nuclear radius and the mass of electron, respectively. We use as usual  $R = r_0 A^{1/3}$  with  $r_0 = 1.2$  fm. Initial and final nuclear ground states with energies  $E_I$  and  $E_F$  are denoted by  $|0_I^+\rangle$  and  $|0_F^+\rangle$ , respectively. The summation runs over intermediate nuclear states  $|n\rangle$  with energies  $E_n$ . The weak one-body nuclear charged current  $J_{L,R}$  [7, 8] depends on the effective value of axial-vector coupling constant  $g_A^{\text{eff}}$  of the nucleon, which is renormalized to a smaller, the so called, ‘‘quenched’’ value,  $g_A^{\text{eff}}$  [10].

### III. ‘‘INTERPOLATING’’ FORMULA FOR THE $0\nu\beta\beta$ -DECAY HALF-LIFE

For the Majorana neutrino exchange mechanism in the literature there usually considered two limiting cases: light  $m_i \ll p_F$  and heavy  $M_i \gg p_F$  neutrinos, where  $p_F \sim 200$  MeV is the Fermi momentum. For these limiting cases the half-life formula (8) is reduced to:

$$\begin{aligned} [T_{1/2}^{0\nu}]^{-1} &= G^{0\nu} g_A^4 \times \\ &\times \begin{cases} |\eta_\nu|^2 |M_\nu^{\prime 0\nu}|^2, & \text{for } m_i \ll p_F, \\ |\eta_N|^2 |M_N^{\prime 0\nu}|^2, & \text{for } M_k \gg p_F, \end{cases} \end{aligned} \quad (9)$$

Table I. The values of the parameter  $\sqrt{\langle p^2 \rangle}$  of the interpolating formula (13), (14) for a given isotope and their average value  $\sqrt{\langle p^2 \rangle}_a$  used in Eq. (17) with the variance  $\sigma$  (in parentheses) calculated within different nuclear structure approaches: interacting shell model (ISM) (Strasbourg-Madrid (StMa)[16] and Central Michigan University (CMU)[17] groups), interacting boson model (IBM)[18], quasiparticle random phase approximation (QRPA) (Tuebingen-Bratislava-Caltech (TBC)[19, 20] and Jyväskylä (Jy)[21] groups), projected Hartree-Fock Bogoliubov approach (PHFB)[22], and covariant density functional theory (CDFT) [23]. The Argonne, CD-Bonn and UCOM two-nucleon short-range correlations are taken into account. The non-quenched value of weak axial-vector coupling  $g_A$  is assumed.

Method	$g_A$	src	$\sqrt{\langle p^2 \rangle}$ [MeV]												$\sqrt{\langle p^2 \rangle}_a$ ( $\sigma$ ) [MeV]
			<sup>48</sup> Ca	<sup>76</sup> Ge	<sup>82</sup> Se	<sup>96</sup> Zr	<sup>100</sup> Mo	<sup>110</sup> Pd	<sup>116</sup> Cd	<sup>124</sup> Sn	<sup>128</sup> Te	<sup>130</sup> Te	<sup>136</sup> Xe	<sup>150</sup> Nd	
ISM-StMa	1.25	UCOM	178	150	149					160		161	159		160(10)
ISM-CMU	1.27	Argonne	178	134	138					153		159	170		155(17)
		CD-Bonn	203	165	162					177		184	197		181(17)
IBM	1.27	Argonne	113	103	103	129	136	135	130	109	109	109	107	155	120(17)
QRPA-TBC	1.27	Argonne	189	163	164	180	174	166	157	186	178	180	183		175(11)
		CD-Bonn	231	193	194	211	204	194	182	214	207	209	211		205(13)
QRPA-Jy	1.26	CD-Bonn		191	192	217	207	187	177	202	196	201	175		194(13)
PHFB	1.25	Argonne				130	127	124			131	132		121	128(4)
		CD-Bonn				150	145	143			150	150		139	146(5)
CDFT	1.25	Argonne	122	129	131	129	131		133	138		138	137	138	132(5)

with

$$\begin{aligned}
|\eta_\nu|^2 m_e^2 &= \left| \sum_{j=1}^3 U_{ej}^2 m_j \right|^2 + \lambda^2 \left| \sum_{j=1}^3 T_{ej}^2 m_j \right|^2 \\
&\simeq \left| \sum_{i=1}^3 U_{ej}^2 m_j \right|^2 \\
|\eta_N|^2 \frac{1}{m_p^2} &= (|\eta_N^L|^2 + |\eta_N^R|^2) \frac{1}{m_p^2} \\
&= \left| \sum_{k=1}^n S_{ek}^2 \frac{1}{M_k} \right|^2 + \lambda^2 \left| \sum_{k=1}^n V_{ek}^2 \frac{1}{M_k} \right|^2 \quad (10)
\end{aligned}$$

Here the NMEs  $M_\nu^{i0\nu}$ ,  $M_N^{i0\nu}$  are derived from the NME  $M^{i0\nu}$  in Eq. (8) in the following way

$$M^{i0\nu}(m_i \rightarrow 0) = \frac{1}{m_p m_e} M_\nu^{i0\nu}, \quad (11)$$

$$M^{i0\nu}(M_i \rightarrow \infty) = \frac{1}{M_i^2} M_N^{i0\nu}. \quad (12)$$

In the case of a neutrino spectrum with mass states  $N_k$  of an arbitrary mass value one has to apply Eq. (8) for the NME calculations, resulting in a complicated function of the neutrino mass. This is a real hassle for use in practice. Fortunately, there is a very good approximate analytical representation for Eq. (8) proposed in Ref. [8] (and references therein) and having a remarkably simple form

$$M_{LL,RR}^{i0\nu}(m_\nu) \simeq M_N^{i0\nu} \frac{1}{\sqrt{\langle p^2 \rangle} + m_\nu^2} \quad (13)$$

This is what we call ‘‘interpolating formula’’ (IntF) since it interpolates two limiting cases (11), (12) and is valid

to a good accuracy for an arbitrary value of  $m_\nu$ . Eq. (13) contains the parameter

$$\langle p^2 \rangle = m_p m_e \frac{M_N^{i0\nu}}{M_\nu^{i0\nu}} \quad (14)$$

with the dimension of (mass)<sup>2</sup>. The form of Eq. (13) suggests the interpretation of  $\langle p^2 \rangle$  as the mean square momentum of the virtual neutrino propagating between two  $\beta$ -decaying nucleons. Therefore, it is expected to be of the order of  $p_F^2 \sim (200 \text{ MeV})^2$ . The current values of the matrix elements  $M_\nu^{i0\nu}$  and  $M_N^{i0\nu}$  calculated within different nuclear structure approaches can be found in Tables 6 and 7 of Ref. [10]. The value of corresponding parameter  $\sqrt{\langle p^2 \rangle}$  is given for various isotopes together with its averaged value  $\sqrt{\langle p^2 \rangle}_a$  with variance  $\sigma$  in Table I. The unquenched value of axial-vector coupling constant is assumed:  $g_A^{\text{eff}} = g_A = 1.25 - 1.27$ . We see that the value of  $\sqrt{\langle p^2 \rangle}$  depends noticeable on the chosen nuclear structure method and considered choice of two-nucleon short-range correlation function. The values of  $\sqrt{\langle p^2 \rangle}_a$  are displayed for different nuclear structure approaches and types of two-nucleon short-range correlations in Fig. 1. The largest value of the parameter  $\sqrt{\langle p^2 \rangle}_a \simeq 200 \text{ MeV}$  is found for the QRPA with isospin restoration and CD-Bonn two-nucleon short range correlations. Surprisingly, within all the considered nuclear structure approaches the variance  $\sigma$  is very small being of the order of 3-10 %, i.e. the value of  $\langle p^2 \rangle$  is *practically the same for all isotopes of experimental interest* and can be replaced with averaged value  $\langle p^2 \rangle_a$ . In Appendix we discuss this finding from the view point of the analytical properties of the NME in Eq. (8) as a function in the complex plane of  $m_\nu$ . The above conclusion is also supported by the statistical treatment of  $M_\nu^{i0\nu}$  and  $M_N^{i0\nu}$  NMEs performed in Ref. [11].

Using the parameter  $\langle p^2 \rangle_a$  in the “interpolating formula” (13) we can write to a good accuracy the  $0\nu\beta\beta$ -decay half-life for the Majorana neutrino exchange mechanism as

$$[T_{1/2}^{0\nu}]^{-1} = \eta_{\nu N}^2 C_{\nu N}, \quad (15)$$

where

$$C_{\nu N} = g_A^4 |M_{\nu}^{0\nu}|^2 G^{0\nu}. \quad (16)$$

and

$$\begin{aligned} \eta_{\nu N}^2 = & \left| \sum_j^3 U_{ej}^2 \frac{m_j}{m_e} + \sum_k^n S_{ek}^2 \frac{\langle p^2 \rangle_a}{\langle p^2 \rangle_a + M_k^2} \frac{M_k}{m_e} \right|^2 \\ & + \lambda^2 \left| \sum_j^3 T_{ej}^2 \frac{m_j}{m_e} + \sum_k^n V_{ek}^2 \frac{\langle p^2 \rangle_a}{\langle p^2 \rangle_a + M_k^2} \frac{M_k}{m_e} \right|^2 \end{aligned} \quad (17)$$

for arbitrary mass  $M_k$ . The sum runs over  $j = 1, 2, 3$  and  $k = 1, \dots, n$ . The values of parameter  $C_{\nu N}$  are given for various isotopes in Table II. The “interpolating formula” in Eq. (15) reproduces the “exact” QRPA result with rather good accuracy except for the transition region where its deviation, as seen from Fig. 8, amounts 20% - 25%. The parameter  $\eta_{\nu N}$  is a general LNV parameter for the light and heavy neutrino mass mechanisms, which is practically independent of the isotope under consideration.

#### IV. LIGHT VS HEAVY NEUTRINO MASS MECHANISMS

From the conclusion of the previous section and Eq. (17) it follows that contrary to the previous expectations in the literature (see for instance Refs. [12, 13]) the dominance of light or heavy neutrino mechanisms of  $0\nu\beta\beta$ -decay cannot be recognized just by observation of this process with different isotopes. An additional theoretical or experimental input about neutrino masses and mixing is needed to shed light on the particular role of each of these mechanisms.

Let us give a couple of examples of model inputs allowing us to distinguish two above-mentioned mechanisms.

For a scenario with three SM singlet neutrinos  $\nu_{e,\mu,\tau R}$  the  $6 \times 6$  mixing matrix  $\mathcal{U}$  in Eq. (5) is completely parameterized with 15 angles, 10 Dirac and 5 Majorana CP violating phases. Let consider some viable structures of this mixing matrix.

##### A. Uncoupled light and heavy neutrino sectors

In the particular case of

$$\mathcal{U} = \begin{pmatrix} U_0 & \mathbf{0} \\ \mathbf{0} & V_0 \end{pmatrix}. \quad (18)$$

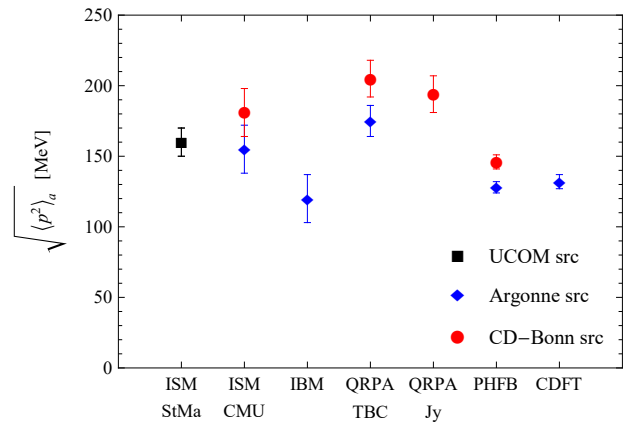


Figure 1. The average value  $\sqrt{\langle p^2 \rangle_a}$  over the set of the considered isotopes with variance  $\sigma$  calculated within different nuclear structure approaches. The notations are the same as in Table I.

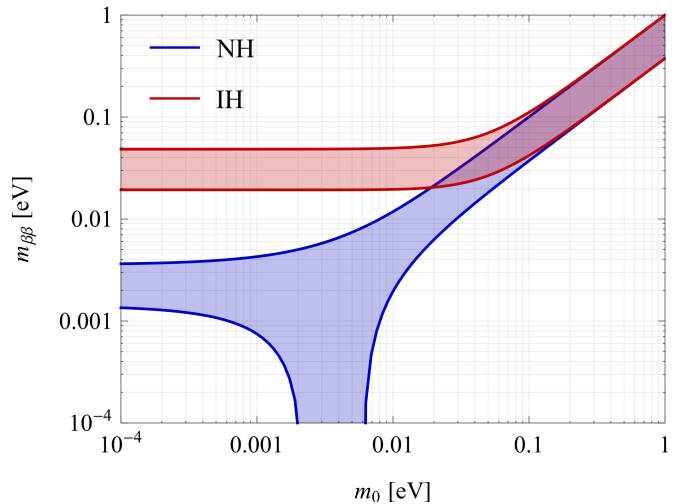


Figure 2. Scenario IV A with  $m_i M_i = \text{const.}$  The effective Majorana neutrino mass  $m_{\beta\beta}$  as a function of the lightest neutrino mass for the normal (blue) and inverted (red) hierarchy of neutrino masses. The best fit values of neutrino oscillation parameters from the global analysis of neutrino oscillation data [24] are considered.

there is no mixing between heavy and light neutrino sectors. Then we have

$$\eta_{\nu N}^2 = \frac{1}{m_e^2} (m_{\beta\beta}^2 + (M_{\beta\beta}^R)^2) \quad (19)$$

$$m_{\beta\beta} = \left| \sum_{j=1}^3 U_{ej}^2 \frac{m_j}{1 + m_j^2/\langle p^2 \rangle_a} \right| \simeq \left| \sum_{j=1}^3 U_{ej}^2 m_j \right|, \quad (20)$$

$$M_{\beta\beta}^R = \lambda \left| \sum_{k=1}^3 U_{ek}^2 \frac{M_k}{1 + M_k^2/\langle p^2 \rangle_a} \right| \simeq \lambda \langle p^2 \rangle_a \left| \sum_{k=1}^3 U_{ek}^2 \frac{1}{M_k} \right|. \quad (21)$$

Table II. The value of the parameter  $C_{\nu N}$  in Eq. (16) for the isotopes of experimental interest. The calculated light neutrino exchange NME  $M'_{\nu}$  within the interacting shell model (ISM) (Strasbourg-Madrid (StMa)[16] and Central Michigan University (CMU)[17] groups), interacting boson model (IBM)[18], quasiparticle random phase approximation (QRPA) (Tuebingen-Bratislava-Caltech (TBC)[19, 20] and Jyväskylä (Jy)[21] groups), projected Hartree-Fock Bogoliubov approach (PHFB)[22] and covariant density functional theory (CDFT) [23] are considered. The Argonne, CD-Bonn and UCOM two-nucleon short-range correlations are taken into account. The non-quenched value of the weak axial-vector coupling  $g_A$  is assumed.

Method	$g_A$	src	$C_{\nu N}$ ( $10^{-14}$ yrs $^{-1}$ )											
			$^{48}\text{Ca}$	$^{76}\text{Ge}$	$^{82}\text{Se}$	$^{96}\text{Zr}$	$^{100}\text{Mo}$	$^{110}\text{Pd}$	$^{116}\text{Cd}$	$^{124}\text{Sn}$	$^{128}\text{Te}$	$^{130}\text{Te}$	$^{136}\text{Xe}$	$^{150}\text{Nd}$
ISM-StMa	1.25	UCOM	4.38	4.56	17.3					15.1	24.4	17.1		
ISM-CMU	1.27	Argonne	4.12	6.96	26.8					9.38	11.8	10.0		
		CD-Bonn	4.98	7.81	30.3					10.8	13.7	11.7		
IBM	1.27	Argonne	19.7	13.4	36.7	42.7	73.5	20.5	41.6	23.9	2.56	50.5	35.2	27.0
QRPA-TBC	1.27	Argonne	1.88	16.3	56.7	39.5	120.	41.4	70.7	15.4	3.17	55.8	18.0	
		CD-Bonn	2.24	19.0	66.4	46.8	141.	48.9	81.6	19.9	3.93	70.4	22.9	
QRPA-Jy	1.26	CD-Bonn		16.5	35.6	51.1	61.0	51.6	76.4	64.0	3.59	57.3	31.1	
PHFB	1.25	Argonne				40.5	132.	59.6			2.18	50.4		23.7
		CD-Bonn				44.6	143.	64.7			2.39	55.0		25.6
CDFT	1.25	Argonne	47.3	22.4	74.0	216.	173.		128.	42.3		88.2	68.0	113.

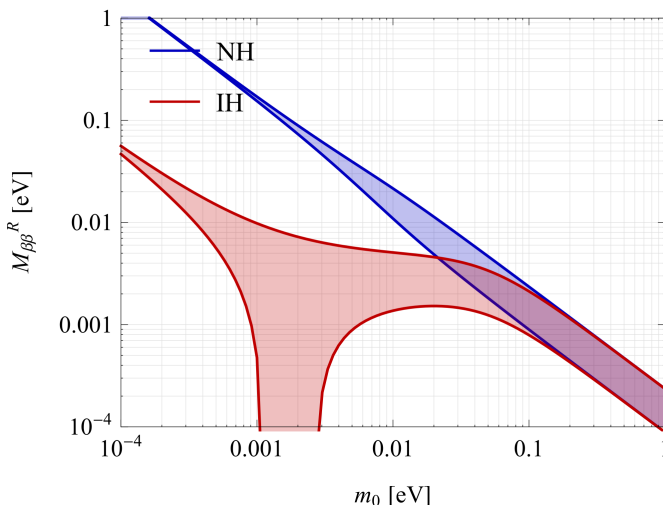


Figure 3. Scenario IV A with  $m_i/M_i = \text{const.}$  The effective Majorana neutrino mass  $M_{\beta\beta}^R$  as a function of the lightest neutrino mass  $m_0$  for the normal (blue) and inverted (red) hierarchy of neutrino masses.

In this scenario  $U_0$  can be identified with the PMNS mixing matrix  $U$ . Thus we assume  $U_0 = U$ . The mixing matrix  $V_0$  for the heavy neutrinos is unknown, but it is similar to  $U_0$  in the light neutrino sector, then  $V_0 = U$  is frequently assumed. For sake of simplicity we consider two different cases for the heavy neutrino masses:

$$M_i = \begin{cases} m_i/\zeta_r & \text{constant ratios} \\ \zeta_p/m_i & \text{constant products} \end{cases} \quad (22)$$

In the case of the constant products  $\zeta_p = m_i M_i$  we have for the LNV parameter in Eq. (19):

$$\eta_{\nu N}^2 = \frac{1}{m_e^2} \left( 1 + \lambda^2 \left( \frac{\langle p^2 \rangle_a}{\zeta_p} \right)^2 \right) m_{\beta\beta}^2 \equiv \kappa^2 m_{\beta\beta}^2. \quad (23)$$

Thus, in this scenario the presence of heavy neutrinos leads to a vertical shift of the standard plot in Fig. 2 by a constant factor  $\kappa$ . As a result, the  $0\nu\beta\beta$ -decay experimental upper bound on  $m_{\beta\beta}$  is significantly less stringent, if  $\zeta_p \ll \lambda \langle p^2 \rangle_a \simeq 24$  MeV $^2$ . In our estimation we used the upper-bound-value in (3), i. e.  $\lambda = 7.7 \cdot 10^{-4}$ , and  $\sqrt{\langle p^2 \rangle_a} = 175$  MeV calculated within the QRPA by assuming Argonne potential and  $g_A = 1.27$  (see Table II).

In the case of the constant ratios  $\zeta_r = m_i/M_i$  in Eq. (22) the effective Majorana neutrino mass  $M_{\beta\beta}$  is shown in Fig. 3. Contribution of  $M_{\beta\beta}$  becomes comparable to  $m_{\beta\beta}$  as soon as  $\zeta_r = 10^{-17}$ , which corresponds to  $M_i \sim 10^{16}$  eV =  $10^4$  TeV.  $\lambda = 7.7 \cdot 10^{-4}$  is assumed again. Notice the reversed behavior of the mass hierarchies: NH no longer exhibits a region unbounded from below, while IH does.

## B. Seesaw-mixed light and heavy neutrino sectors

Assuming for simplicity the flavor universal mixing between the active and sterile neutrino sectors the seesaw mixing matrix  $\mathcal{U}$  takes the form

$$\mathcal{U} = \begin{pmatrix} U_0 & \zeta \mathbf{1} \\ -\zeta \mathbf{1} & V_0 \end{pmatrix}. \quad (24)$$

Here,  $\zeta = \frac{m_D}{m_{LNV}}$ , where  $m_D$  is the typical scale of the charged leptons masses and  $m_{LNV}$  is the LNV scale of

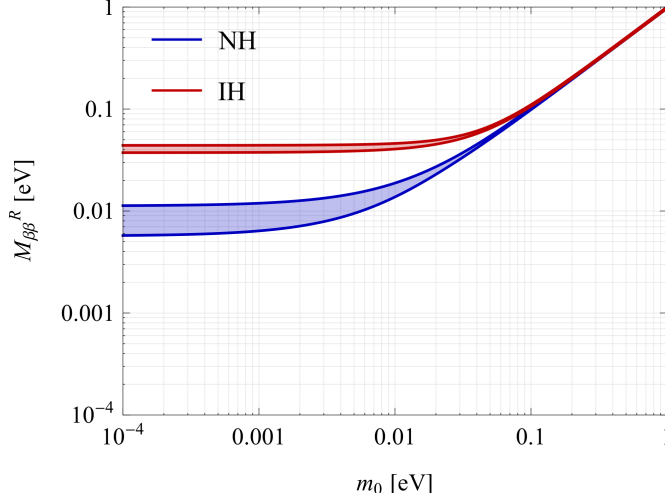


Figure 4. Scenario IV B. The effective Majorana neutrino mass  $M_{\beta\beta}^R$  in Eq. (29) with  $m_D = 5$  MeV as a function of the lightest neutrino mass  $m_0$  for the normal (blue) and inverted (red) hierarchy of neutrino masses.

$$V_0 = U_0^\dagger = \begin{pmatrix} c_{12} c_{13} e^{-i\alpha_1} & (-s_{12} c_{23} - c_{12} s_{13} s_{23} e^{-i\delta}) e^{-i\alpha_1} & (s_{12} s_{23} - c_{12} s_{13} c_{23} e^{-i\delta}) e^{-i\alpha_1} \\ s_{12} c_{13} e^{-i\alpha_2} & (c_{12} c_{23} - s_{12} s_{13} s_{23} e^{-i\delta}) e^{-i\alpha_2} & (-c_{12} s_{23} - s_{12} s_{13} c_{23} e^{-i\delta}) e^{-i\alpha_2} \\ s_{13} e^{i\delta} & c_{13} s_{23} & c_{13} c_{23} \end{pmatrix}. \quad (27)$$

We note that each element of the first row is multiplied by the same phase factor  $e^{-i\alpha_1}$ . Analogously, the second row is multiplied by  $e^{-i\alpha_2}$ . Therefore, the Majorana phases  $\alpha_{1,2}$  do not affect the heavy neutrino LNV parameter  $M_{\beta\beta}^R$  in this case. On the contrary, the Dirac phase  $\delta$ , which does not affect the light neutrino LNV parameter  $m_{\beta\beta}$  will impact the value of  $M_{\beta\beta}^R$ . The seesaw structure of (24) implies  $m_i \simeq m_D^2/m_{LNV}$  and  $M_i \simeq m_{LNV}$ . For a product of light and heavy neutrino masses let assume  $m_i M_i \simeq m_D^2$ . If the LNV scale is significantly larger than  $\langle p^2 \rangle_a$  we find

$$\eta_{\nu N}^2 = \frac{1}{m_e^2} (m_{\beta\beta}^2 + (M_{\beta\beta}^R)^2) \quad (28)$$

with

$$M_{\beta\beta}^R = \lambda \frac{\langle p^2 \rangle_a}{m_D^2} \left| \sum_{j=1}^3 (U_0^\dagger)_{ej}^2 m_j \right|. \quad (29)$$

We note that for  $m_D \simeq 5$  MeV the coefficient  $\lambda \langle p^2 \rangle_a / m_D^2$  entering  $M_{\beta\beta}^R$  in Eq. (29) is close to unity and it might be that contributions from the light and heavy neutrinos to  $\eta_{\nu N}$  are comparable. However,  $M_{\beta\beta}^R$  is not proportional to  $m_{\beta\beta}$  as off-diagonal elements of matrices  $U_0$  and  $(U_0^\dagger)$  are different. Therefore, a detailed analysis is needed to establish an useful constraint on the Yukawa potential associated with neutrinos. In

the order of the Majorana masses  $M_i$  of the heavy neutrinos. As in the previous scenario  $U_0$  can be identified with the PMNS  $U$  matrix. Thus we assume  $U = U_0$ . For  $V_0$ , analogue of  $U_0$  in the heavy neutrino sector, we find from the unitarity conditions

$$V_0 = U_0^\dagger \quad (25)$$

and

$$U_0 U_0^\dagger = (1 - \zeta^2) \mathbf{1}, \quad V_0 V_0^\dagger = (1 - \zeta^2) \mathbf{1}. \quad (26)$$

It is assumed that a small violation of the unitarity of  $U_0$  and  $V_0$  matrices is beyond the current accuracy of phenomenological determination of elements of the PMNS matrix. The matrix  $V_0$  takes the form

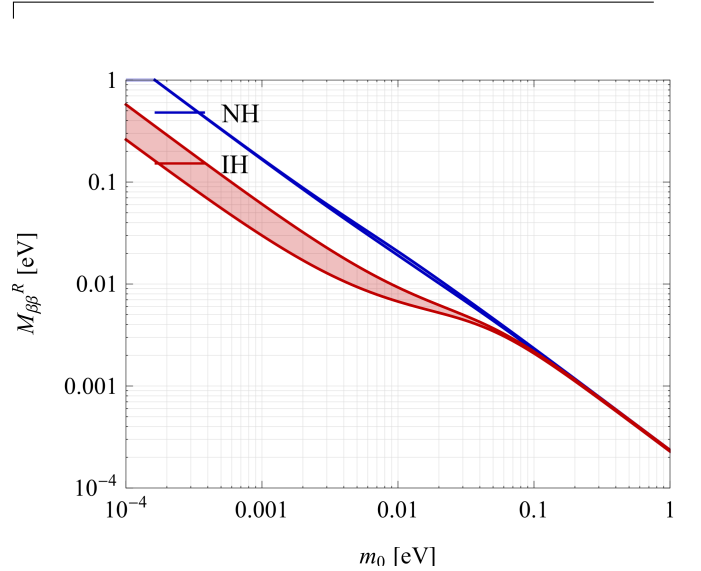


Figure 5. The same as in Fig. 4, but for  $M_{\beta\beta}^R$  defined according to Eq. (30) with  $\zeta^2 = 10^{-17}$ .

Fig. 4 we show  $M_{\beta\beta}^R$  as function of lightest neutrino mass both for normal and inverted hierarchy by assuming  $m_D \simeq 5$  MeV (and  $\lambda = 7.7 \cdot 10^{-4}$ ).

Within the seesaw structure one can also assume

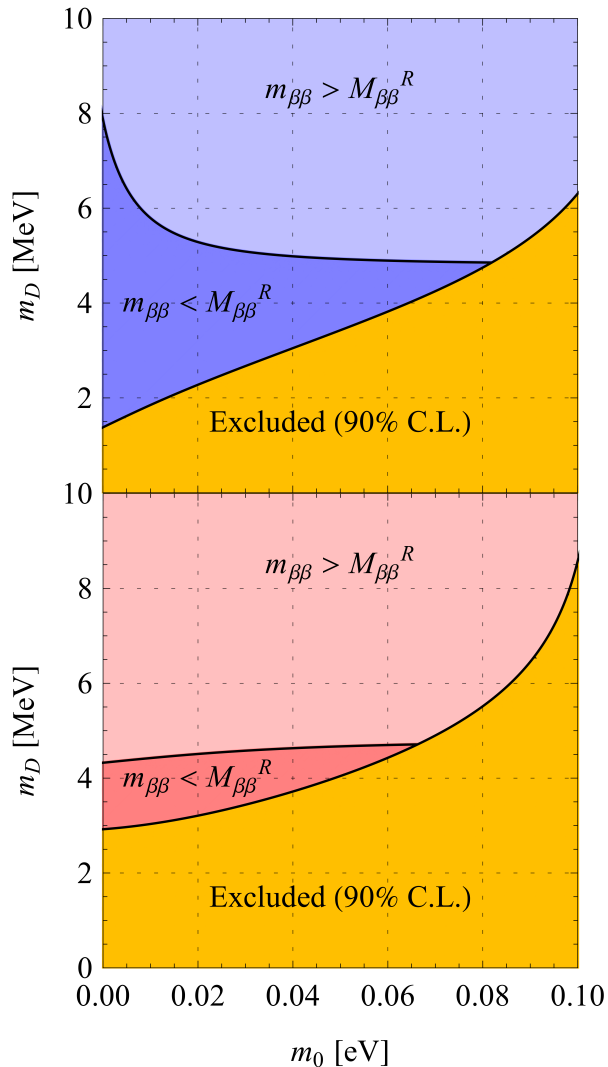


Figure 6. Scenario IVB with the mass relation  $m_i \simeq m_D^2/M_i$ . The comparison of the light  $m_{\beta\beta}$  and heavy  $M_{\beta\beta}^R$  neutrino contributions to  $0\nu\beta\beta$ -decay for the normal(inverted) hierarchy is shown in left(right) panel.

$m_i \simeq \zeta^2 M_i$ . Then we find

$$M_{\beta\beta}^R = \lambda \zeta^2 \left| \sum_{j=1}^3 (U_0^\dagger)_{ej}^2 \frac{\langle p^2 \rangle_a}{m_j} \right|. \quad (30)$$

For  $\zeta^2 = 10^{-17}$  and  $\lambda = 7.7 \cdot 10^{-4}$  the effective mass  $M_{\beta\beta}^R$  in Eq. (30) is plotted in Fig. 5. We see again that for a chosen set of parameters the value of  $M_{\beta\beta}^R$  can be comparable with  $m_{\beta\beta}$  (see Fig. 2).

In Table III we show upper bounds on  $\eta_{\nu N}$  in Eq. (28) derived from the current  $0\nu\beta\beta$ -decay experiments. As seen, the most stringent bound comes out from  $^{136}\text{Xe}$   $0\nu\beta\beta$ -decay experiment Ref. [31]. For this bound we analyzed the separate contributions of the light and heavy neutrinos to  $0\nu\beta\beta$ -decay. Fig. 6 displays the corresponding results in the plane of the parameters  $m_D$  and  $m_0$  ( $m_i \simeq m_D^2/M_i$  is assumed) for the cases of the normal

(left panel) and inverted hierarchy (right panel) of neutrino masses. We see that in the considered scenario for normal (inverted) hierarchy the values  $m_D \leq 1.5$  MeV ( $m_D \leq 2.9$  MeV) are already excluded by the existing experimental data on  $0\nu\beta\beta$ -decay. We also see that in the case of normal (inverted) neutrino mass hierarchy the heavy neutrino exchange mechanism cannot dominate over the light one in the region  $m_0 \geq 0.08$  eV ( $m_0 \geq 0.065$  eV). The constraint from the  $0\nu\beta\beta$ -decay experiment imply that the limit on the mass of lightest heavy neutrino is  $M_3 > 38$  TeV and  $M_2 > 171$  TeV in the cases of normal and inverted hierarchy, respectively.

Fig. 7 shows results of an analysis similar to the above-discussed one, but for  $\zeta^2 = m_i/M_i$  scenario. In this case the heavy neutrino mechanism cannot dominate in practically the same domain of  $m_0$  as previously. It is concluded that in the case of normal (inverted) hierarchy  $\zeta \leq 1.75 \times 10^{-8}$  ( $\zeta \leq 1.65 \times 10^{-8}$ ). We note that within the considered seesaw scenario within the LRSM the effective Majorana neutrino mass  $m_{\beta\beta}$  can not be identified with the first element of the Dirac-Majorana mass (see Appendix B)  $(M_L)_{ee}$ , which contains additional term  $\zeta^2 M_1$  in magnitude comparable with  $m_1$ . The corresponding term in  $m_{\beta\beta}$  has been neglected as it is suppressed by properties of neutrino propagator for large neutrino mass. Due to the same reason  $M_{\beta\beta}$  can not be identified with  $(M_R)_{ee}$ .

## V. CONCLUSIONS

In summary, we have shown that the ratio of nuclear matrix elements for the light and heavy neutrino mass mechanisms exhibits practically no dependence on isotope for all favoured nuclear structure methods. This quantity, when properly scaled, can be identified with squared average neutrino momentum  $\langle p^2 \rangle$  of the interpolating formula including light and heavy neutrino exchange mechanisms. The universality of the averaged value of  $\langle p^2 \rangle$  for a set of isotopes allows determination of a new LNV parameter  $\eta_{\nu N}$ , which is a coherent sum of squared LNV parameters  $m_{\beta\beta}$  and  $M_{\beta\beta}^R$  characterizing the light and heavy neutrino exchange mechanisms, respectively. Thus, the observation of  $0\nu\beta\beta$ -decay on two and more nuclear isotopes will allow one to deduce information about the size of  $\eta_{\nu N}$ , but not about the relative contribution of light or heavy neutrino-exchange mechanism to the decay rate. An additional theoretical or experimental input about neutrino masses and mixing is needed to shed light on the particular role of each of these mechanisms. As an example we considered a simplified see-saw type  $6 \times 6$  neutrino mixing matrix (24), which implies that the  $3 \times 3$  mixing matrix of heavy neutrinos is the hermitian conjugate of the  $3 \times 3$  PMNS mixing matrix of light neutrinos. Assuming several viable seesaw relations among the light  $m_i$  and heavy  $M_i$  neutrino masses ( $i=1,2$  and 3) useful constraints on the parameters, in particular Dirac neutrino mass  $m_D$ , entering these relations have been

Table III. Upper bounds on the effective lepton number violating parameter  $\eta_{\nu N}$  imposed by the current constraints on the  $0\nu\beta\beta$ -decay half-life  $T_{1/2}^{0\nu-exp}$  (the first row). The values in the second and the third rows were obtained using the largest and lowest values of  $C_{\nu N}$  for a given isotope from Table II, respectively.

	$^{48}\text{Ca}$	$^{76}\text{Ge}$	$^{82}\text{Se}$	$^{100}\text{Mo}$	$^{116}\text{Cd}$	$^{130}\text{Te}$	$^{136}\text{Xe}$
$T_{1/2}^{0\nu-exp}$ [yrs]	$2.0 \times 10^{22}$ [25]	$5.3 \times 10^{25}$ [26]	$2.5 \times 10^{23}$ [27]	$1.1 \times 10^{24}$ [28]	$1.7 \times 10^{23}$ [29]	$4.0 \times 10^{24}$ [30]	$1.07 \times 10^{26}$ [31]
$\eta_{\nu N} \times 10^6$	10.3	0.290	2.32	0.724	2.14	0.532	0.117
	33.8	0.643	4.81	1.22	3.76	1.455	0.306

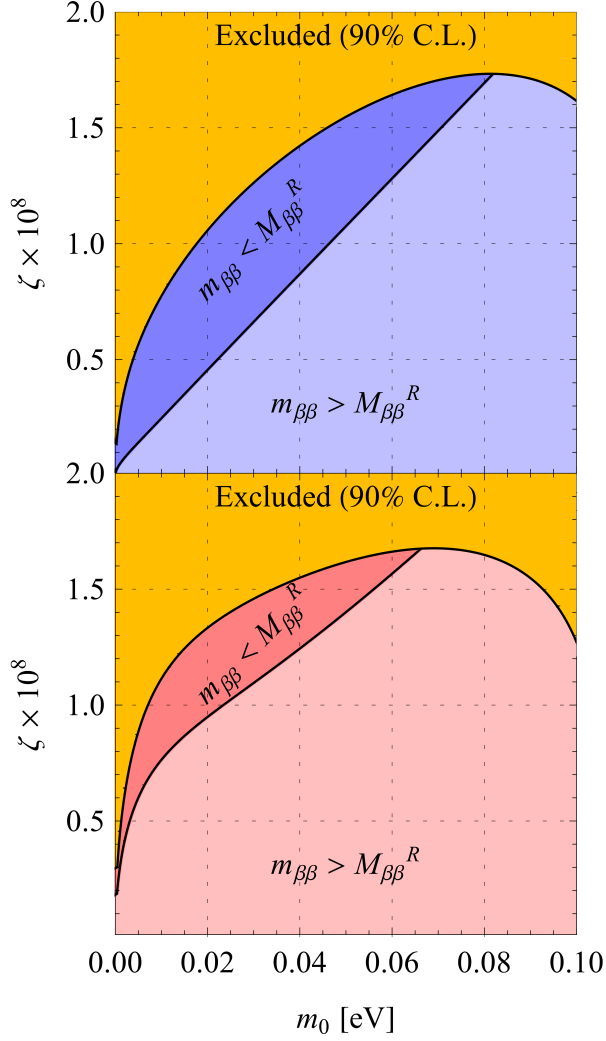


Figure 7. The same as in Fig. 6, but with the mass relation  $\zeta^2 = m_i/M_i$ .

obtained from the experimental lower bounds on the  $0\nu\beta\beta$ -decay half-life. The region of dominance of heavy over light neutrino exchange mechanisms for the considered scenarios have been identified.

## ACKNOWLEDGMENTS

This work is supported by the VEGA Grant Agency of the Slovak Republic under Contract No. 1/0922/16, by Slovak Research and Development Agency under Contract No. APVV-14-0524, RFBR Grants Nos. 16-02-01104 and 18-02-00733, Underground laboratory LSM - Czech participation to European-level research infrastructure CZ.02.1.01/0.0/0.0/16\_013/0001733, Fondecyt (Chile) grant No. 1150792, and by CONICYT (Chile) Ring ACT1406, PIA/Basal FB0821.

## Appendix A: Analytical Properties of the NMEs and the Interpolating formula

Here we give some comments on the possible improvement of our interpolating formula in Eq. (13), which we call the “monopole” approximation. Numerically the latter is already a very good approximation to the “exact” NMEs given by Eq. (8) and calculated in the framework of any specific nuclear structure approach. However in certain cases one may need an approximate formula having not only a good numerical precision, but also the analytical properties in the complex plane of  $m_\nu$  the same or maximally close to the “exact” NME defined in expression (8).

Obviously the monopole approximation (13) has two imaginary poles in the complex plane of  $m_\nu$ , while they are absent in the exact expression (8). Below we describe a class of approximations with the analytic properties of the “exact” NME (8).

Let us rewrite Eq. (8) in the form

$$M_{LL,RR}^{0\nu}(m_\nu) = \frac{4\pi}{(2\pi)^3} \int_0^\infty p^2 dp \frac{\varphi(p)}{E_p(E_p + \Delta)}, \quad (\text{A1})$$

where  $\Delta = E_n - (E_I - E_F)/2 > 0$ ,  $E_p = \sqrt{p^2 + m_\nu^2}$ ,

$$\varphi(p) = \int d\mathbf{x} d\mathbf{y} e^{i\mathbf{p}\cdot(\mathbf{x}-\mathbf{y})} \varphi(\mathbf{x}, \mathbf{y}), \quad (\text{A2})$$

and

$$\varphi(\mathbf{x}, \mathbf{y}) = \frac{1}{m_p m_e} \frac{4\pi R}{g_A^2} \sum_n \langle 0_F^+ | J_{LR}^{\mu\dagger}(\mathbf{x}) | n \rangle \langle n | J_{\mu LR}^\dagger(\mathbf{y}) | 0_i^+ \rangle. \quad (\text{A3})$$



The function  $\varphi(\mathbf{x}, \mathbf{y})$  describes a distribution of currents inside the nucleus. In Eq. (A1) the neutrino mass enters the denominator of the integrand.

Analytic properties of functions defined in terms of a contour integral are fixed by the Landau rules [33, 34].

The singular points of the first kind are associated with singular behavior of the integrand at the end points of the integration contour. In the case of Eq. (A1), these singularities could occur provided that  $\chi(p) \equiv E_p(E_p + \Delta) = 0$  for  $p = 0$  or  $\infty$ . This equation can be fulfilled for  $p = 0$  only to give  $m = 0$  and  $m = \pm\Delta$ . The points  $m = \pm\Delta$  are located on the different sheets of the Riemann surface of  $M'_{LL,RR}{}^{0\nu}(m_\nu)$ . It is clear that model dependent features of the nuclear structure entering  $\varphi(\mathbf{x}, \mathbf{y})$  do not affect the end point singularities.

Singular points of the second kind are associated with the pinch singularities of the integrand. To find them, the equations  $\chi(p)/\varphi(p) = 0$  and  $(\chi(p)/\varphi(p))' = 0$  are to be solved, which localise high-order poles of the integrand in the complex  $p$ -plane. These singularities depend on  $\varphi(\mathbf{x}, \mathbf{y})$  and thereby on the nuclear structure model.

Analytic properties of  $M'_{LL,RR}{}^{0\nu}(m_\nu)$  as a function of  $\Delta$  are particularly simple. Changing the variable in Eq. (A4) to  $p = m \sinh \theta$ , we arrive at the dispersion integral

$$M'_{LL,RR}{}^{0\nu}(m_\nu) = \frac{4\pi m}{(2\pi)^3} \int_0^\infty \sinh^2 \theta d\theta \frac{\varphi(m \sinh \theta)}{\cosh \theta - \xi}, \quad (\text{A4})$$

where  $\xi = -\Delta/m_\nu$ . This equation shows that  $M'_{LL,RR}{}^{0\nu}$  is an analytic function in the complex  $\xi$ -plane with the cut  $(1, +\infty)$  corresponding to the cut  $(-\Delta, 0)$  in  $m_\nu$ . Provided  $\varphi(p)$  is an analytic function for  $|p| < \infty$  and the integral (A4) converges,  $M'_{LL,RR}{}^{0\nu}(m)$  turns out to be an analytic function in the complex  $m_\nu$ -plane with the cut  $(-\Delta, 0)$ . On the second sheet of the Riemann surface one finds a branch point  $m = +\Delta$ .

As we discussed before the monopole parametrization (13) is numerically very accurate. This parametrization corresponds to an approximation of the spectral function with the delta function:  $\phi_m(p) \sim \delta(p^2 - \langle p^2 \rangle)$ . Then for the formula with the correct analytical properties, which we are going to construct here, we chose the spectral function in a form close to the  $\phi_m(p)$  to guarantee its numerical accuracy comparable with the monopole parameterization. We may choose

$$\phi(p) = \exp\left(-\frac{\rho^2 p^2}{2}\right) \frac{\sinh(\rho^2 p p_0)}{\rho^2 p p_0}. \quad (\text{A5})$$

with the free parameters,  $\rho$  and  $p_0 \sim \langle p^2 \rangle^{1/2}$ , which can be fixed by normalization to the exact values at zero and at infinity. The function  $\phi(p)$  for  $p = p_0$  is close to the maximum, the value of  $1/\rho$  determines the width of momentum distribution. This spectral function is analytic for  $|p| < \infty$  and it generates model independent end-point singularities only. The corresponding interpolating formula appears to be an analytic function in the

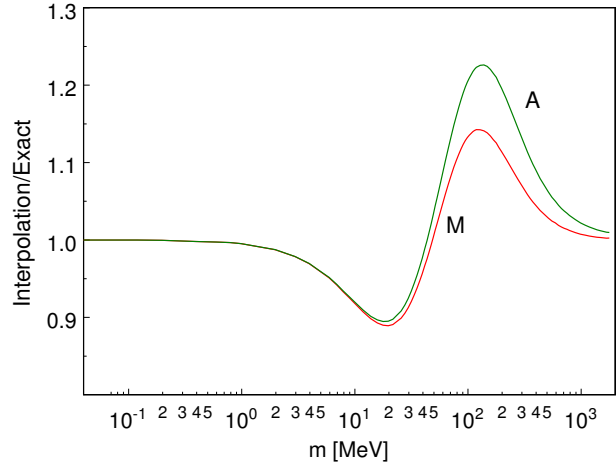


Figure 8. (color online) Ratio between the interpolation formulas and the exact calculation for  ${}^{76}\text{Ge}$  versus neutrino mass. The curve M is for the monopole interpolation (13), the curve A shows the ratio for the analytic interpolation formula.

complex  $m_\nu$ -plane with the cut  $(-\Delta, 0)$ . The cut position is model-independent. The discontinuity depends on  $\phi(p)$  and is model dependent. A particularly strong effect on the behavior of analytic functions in a fixed domain comes from nearest singularities. Taking into account that  $\Delta \sim 10$  MeV, an improved description of the neutrino mass dependence can be expected around zero neutrino mass in the circle with a radius of a few tens of MeV. This scale is smaller than the characteristic momentum transfer  $p_0 \sim 200$  MeV. Reasonable accuracy is also expected for large  $m_\nu$  domain, provided the spectral function (A5) approximates closely the monopole spectral function found to be successful phenomenologically.

The ratio between the interpolating formula of Eq. (13) and the exact calculation for  ${}^{76}\text{Ge}$  is shown on Fig. 8. The result is compared to the interpolating formula of the spectral function (A5) with  $\rho = 5$  fm and  $p_0 = 0.84/\text{fm}$ . For low neutrino masses up to about 40 MeV the analytic interpolation formula approximates the exact result with a better accuracy. For higher masses the nuclear structure at about 200 MeV becomes important, which could reflect a contribution of the model dependent pinch singularities which we do not consider.

## Appendix B: Dirac-Majorana neutrino mass term within seesaw in LRSM

In this Appendix the Dirac-Majorana neutrino mass term associated with the see-saw mass mechanism within the LRSM and particular case of neutrino mixing

given in Eq. (24) is presented. We have

$$\begin{aligned}\mathcal{L}_{D+M} &= -\frac{1}{2} \begin{pmatrix} \overline{\nu'_L} & \overline{\nu'_R} \end{pmatrix} \begin{pmatrix} M_L & M_D \\ M_D^T & M_R \end{pmatrix} \begin{pmatrix} \nu'_L \\ \nu'_R \end{pmatrix} + \text{H.c.} \\ &= -\frac{1}{2} \sum_{i=1}^3 (m_i \overline{\nu'_i} \nu'_i + M_i \overline{N_i} N_i). \end{aligned} \quad (\text{B1})$$

Here,  $\nu'_L = (\nu'_{eL}, \nu'_{\mu L}, \nu'_{\tau L})^T$  and  $\nu'_R = (\nu'_{eR}, \nu'_{\mu R}, \nu'_{\tau R})^T$  are three-component columns of the active left-handed  $\nu'_{\alpha L}$  and sterile right-handed  $\nu'_{\alpha R}$  ( $\alpha = e, \mu, \tau$ ) flavor-neutrino fields, respectively. The elements of the  $6 \times 6$  Dirac-Majorana mass matrix  $\mathcal{M}$  are can be calculated as follows:

$$\begin{aligned}\mathcal{M} &= \begin{pmatrix} M_L & M_D \\ M_D^T & M_R \end{pmatrix} \\ &= \begin{pmatrix} U & \zeta \mathbf{1} \\ -\zeta \mathbf{1} & U^\dagger \end{pmatrix}^* \begin{pmatrix} m & 0 \\ 0 & M \end{pmatrix}^* \begin{pmatrix} U & \zeta \mathbf{1} \\ -\zeta \mathbf{1} & U^\dagger \end{pmatrix}^\dagger \end{aligned} \quad (\text{B2})$$

Here,  $m$  and  $M$  stand for diagonal  $3 \times 3$  mass matrices  $m = \text{diag}(m_1, m_2, m_3)$  and  $M = \text{diag}(M_1, M_2, M_3)$ , respectively. By assuming the see-saw relation  $m_i \sim \zeta^2 M_i$  ( $i=1,2,3$ ) among light and heavy neutrino masses the elements of  $\mathcal{M}$  expressed in terms 3 mixing angles  $\theta_{12}, \theta_{13}, \theta_{23}$ , 3 CP phases  $\alpha_1, \alpha_2, \delta$ , 6 neutrino masses and the seesaw parameter  $\zeta$  are given by

$$\begin{aligned}(M_L)_{ee} &= \zeta^2 M_1 + c_{12}^2 c_{13}^2 e^{-i2\alpha_1} m_1 \\ &\quad + s_{12}^2 c_{13}^2 e^{-i2\alpha_2} m_2 + s_{13}^2 e^{i2\delta} m_3, \\ (M_L)_{e\mu} &= -c_{12} c_{13} (s_{12} c_{23} + c_{12} s_{13} s_{23} e^{-i\delta}) e^{-i2\alpha_1} m_1 \\ &\quad + s_{12} c_{13} (c_{12} c_{23} - s_{12} s_{13} s_{23} e^{-i\delta}) e^{-i2\alpha_2} m_2 \\ &\quad + s_{13} c_{13} s_{23} e^{i\delta} m_3, \\ (M_L)_{e\tau} &= c_{12} c_{13} (s_{12} s_{23} - c_{12} s_{13} c_{23} e^{-i\delta}) e^{-i2\alpha_1} m_1 \\ &\quad - s_{12} c_{13} (c_{12} s_{23} + s_{12} s_{13} c_{23} e^{-i\delta}) e^{-i2\alpha_2} m_2 \\ &\quad + s_{13} c_{13} c_{23} e^{i\delta} m_3, \\ (M_L)_{\mu\mu} &= (s_{12} c_{23} + c_{12} s_{13} s_{23} e^{-i\delta})^2 e^{-i2\alpha_1} m_1 \\ &\quad + (c_{12} c_{23} - s_{12} s_{13} s_{23} e^{-i\delta})^2 e^{-i2\alpha_2} m_2 \\ &\quad + c_{13}^2 s_{23}^2 m_3 + \zeta^2 M_2, \\ (M_L)_{\mu\tau} &= (-s_{12} s_{23} + c_{12} s_{13} c_{23} e^{-i\delta}) \times \\ &\quad (s_{12} c_{23} + c_{12} s_{13} s_{23} e^{-i\delta}) e^{-i2\alpha_1} m_1 \\ &\quad - (c_{12} s_{23} + s_{12} s_{13} c_{23} e^{-i\delta}) \times \\ &\quad (c_{12} c_{23} - s_{12} s_{13} s_{23} e^{-i\delta}) e^{-i2\alpha_2} m_2 \\ &\quad + c_{13}^2 s_{23} c_{23} m_3, \end{aligned}$$

$$\begin{aligned}(M_L)_{\tau\tau} &= (s_{12} s_{23} - c_{12} s_{13} c_{23} e^{-i\delta})^2 e^{-i2\alpha_1} m_1 \\ &\quad + (c_{12} s_{23} + s_{12} s_{13} c_{23} e^{-i\delta})^2 e^{-i2\alpha_2} m_2 \\ &\quad + c_{13}^2 c_{23}^2 m_3 + \zeta^2 M_3, \end{aligned} \quad (\text{B3})$$

$$\begin{aligned}(M_D)_{ee} &= \zeta [-c_{12} c_{13} e^{-i\alpha_1} m_1 + c_{12} c_{13} e^{i\alpha_1} M_1], \\ (M_D)_{e\mu} &= \zeta [-s_{12} c_{13} e^{-i\alpha_2} m_2 + s_{12} c_{13} e^{i\alpha_2} M_1], \\ (M_D)_{e\tau} &= \zeta [-s_{13} e^{i\delta} m_3 + s_{13} e^{-i\delta} M_1], \\ (M_D)_{\mu e} &= \zeta [(s_{12} c_{23} + c_{12} s_{13} s_{23} e^{-i\delta}) e^{-i\alpha_1} m_1 \\ &\quad - (s_{12} c_{23} + c_{12} s_{13} s_{23} e^{i\delta}) e^{i\alpha_1} M_2], \\ (M_D)_{\mu\mu} &= \zeta [-(c_{12} c_{23} - s_{12} s_{13} s_{23} e^{-i\delta}) e^{-i\alpha_2} m_2 \\ &\quad + (c_{12} c_{23} - s_{12} s_{13} s_{23} e^{i\delta}) e^{i\alpha_2} M_2], \\ (M_D)_{\mu\tau} &= \zeta [-c_{13} s_{23} m_3 + c_{13} s_{23} M_2], \\ (M_D)_{\tau e} &= \zeta [-(s_{12} s_{23} - c_{12} s_{13} c_{23} e^{-i\delta}) e^{-i\alpha_1} m_1 \\ &\quad + (s_{12} s_{23} - c_{12} s_{13} c_{23} e^{i\delta}) e^{i\alpha_1} M_3], \\ (M_D)_{\tau\mu} &= \zeta [(c_{12} s_{23} + s_{12} s_{13} c_{23} e^{-i\delta}) e^{-i\alpha_2} m_2 \\ &\quad - (c_{12} s_{23} + s_{12} s_{13} c_{23} e^{i\delta}) e^{i\alpha_2} M_3], \\ (M_D)_{\tau\tau} &= \zeta [-c_{13} c_{23} m_3 + c_{13} c_{23} M_3], \end{aligned} \quad (\text{B4})$$

$$\begin{aligned}(M_R)_{ee} &= \zeta^2 m_1 + c_{12}^2 c_{13}^2 e^{i2\alpha_1} M_1 \\ &\quad + (s_{12} c_{23} + c_{12} s_{13} s_{23} e^{i\delta})^2 e^{i2\alpha_1} M_2 \\ &\quad + (s_{12} s_{23} - c_{12} s_{13} c_{23} e^{i\delta})^2 e^{i2\alpha_1} M_3, \\ (M_R)_{e\mu} &= s_{12} c_{12} c_{13}^2 e^{i(\alpha_1 + \alpha_2)} M_1 \\ &\quad - (s_{12} c_{23} + c_{12} s_{13} s_{23} e^{i\delta}) \times \\ &\quad (c_{12} c_{23} - s_{12} s_{13} s_{23} e^{i\delta}) e^{i(\alpha_1 + \alpha_2)} M_2 \\ &\quad - (s_{12} s_{23} - c_{12} s_{13} c_{23} e^{i\delta}) \times \\ &\quad (c_{12} s_{23} + s_{12} s_{13} c_{23} e^{i\delta}) e^{i(\alpha_1 + \alpha_2)} M_3, \\ (M_R)_{e\tau} &= c_{12} s_{13} c_{13} e^{-i\delta} e^{i\alpha_1} M_1 \\ &\quad - c_{13} (s_{12} s_{23} c_{23} + c_{12} s_{13} s_{23}^2 e^{i\delta}) e^{i\alpha_1} M_2 \\ &\quad + c_{13} (s_{12} s_{23} c_{23} - c_{12} s_{13} c_{23}^2 e^{i\delta}) e^{i\alpha_1} M_3, \\ (M_R)_{\mu\mu} &= \zeta^2 m_2 + s_{12}^2 c_{13}^2 e^{i2\alpha_2} M_1 \\ &\quad + (c_{12} c_{23} - s_{12} s_{13} s_{23} e^{i\delta})^2 e^{i2\alpha_2} M_2 \\ &\quad + (c_{12} s_{23} + s_{12} s_{13} c_{23} e^{i\delta})^2 e^{i2\alpha_2} M_3, \\ (M_R)_{\mu\tau} &= s_{12} s_{13} c_{13} e^{-i\delta} e^{i\alpha_2} M_1 \\ &\quad + c_{13} (c_{12} s_{23} c_{23} - s_{12} s_{13} s_{23}^2 e^{i\delta}) e^{i\alpha_2} M_2 \\ &\quad - c_{13} (c_{12} s_{23} c_{23} + s_{12} s_{13} c_{23}^2 e^{i\delta}) e^{i\alpha_2} M_3, \\ (M_R)_{\tau\tau} &= s_{13}^2 e^{-i2\delta} M_1 + c_{13}^2 s_{23}^2 M_2 \\ &\quad + c_{13}^2 c_{23}^2 M_3 + \zeta^2 m_3. \end{aligned} \quad (\text{B5})$$

We note that due to the seesaw relation  $m_i \sim \zeta^2 M_i$  terms  $\zeta m_i$  and  $\zeta^2 m_i$  entering elements of matrices  $M_D$  and  $M_R$ , respectively, can be safely neglected unlike terms  $\zeta^2 M_i$  appearing in the diagonal elements of the  $M_L$  matrix.

- [3] J.C. Pati and A. Salam, Phys. Rev. D **10**, 275 (1974); R. Mohapatra and J.C. Pati, Phys. Rev. D **11**, 2558 (1975).
- [4] G. Senjanovic and R.N. Mohapatra, Phys. Rev. D **12**, 1502 (1975); R. N. Mohapatra and G. Senjanovic, Phys. Rev. Lett. **44**, 912 (1980); Phys. Rev. D **23**, 165 (1981).
- [5] M. Doi, T. Kotani and E. Takasugi, Prog. Theor. Phys. Supplement **83**, 1 (1985).
- [6] F. Šimkovic, Štefánik, R. Dvornický, PoS NOW2016, 074 (2017).
- [7] D. Štefánik, R. Dvornický, F. Šimkovic, and P. Vogel, Phys. Rev. C **92**, 055502 (2015).
- [8] A. Faessler, M. González, S. Kovalenko, and F. Šimkovic, Phys. Rev. D **90**, 096010 (2014).
- [9] J. Kotila and F. Iachello, Phys. Rev. C **85**, 034316 (2012).
- [10] J. D. Vergados, H. Ejiri, and F. Šimkovic, Int. J. Mod. Phys. E **25**, 1630007 (2016).
- [11] E. Lisi, A.M. Rotunno, and F. Šimkovic, Phys. Rev. D **92**, 093004 (2015).
- [12] A. Faessler, A. Meroni, S. T. Petcov, F. Šimkovic and J. Vergados, Phys. Rev. D **83**, 113003 (2011)
- [13] A. Meroni, S. T. Petcov and F. Šimkovic, JHEP **1302**, 025 (2013).
- [14] Zhi-zhong Xing, Phys. Rev. D **85**, 013008 (2012).
- [15] P.S. Bhupal Dev, S. Goswami and M. Mitra, Phys. Rev. D **91**, 113004 (2015).
- [16] J. Menendez, A. Poves, E. Caurier and F. Nowacki, Nucl. Phys. A **818**, 139 (2009).
- [17] M. Horoi and A. Neacsu, Phys. Rev. C **93**, 024308 (2016).
- [18] J. Barea, J. Kotila and F. Iachello, Phys. Rev. C **91**, 034304 (2015).
- [19] F. Šimkovic, V. Rodin, A. Faessler and P. Vogel, Phys. Rev. C **87**, 045501 (2013).
- [20] D. Fang, A. Faessler and F. Šimkovic, Phys. Rev. C **92**, 044301 (2015).
- [21] J. Hyvärinen and J. Suhonen, Phys. Rev. C **91** (2015) 024613.
- [22] P. Rath, R. Chandra, P. Raina, K. Chaturvedi and J. Hirsch, Phys. Rev. C **85**, 014308 (2012).
- [23] L.S. Song, J.M. Yao, P. Ring, and J. Meng, Phys. Rev. C **95**, 024305 (2017).
- [24] F. Capozzi, E. Lisi, A.,Marrone, D. Montanino, and A. Palazzo, Nucl. Phys. B **908**, 218 (2016).
- [25] The NEMO-3 Collab., R. Arnold et al., Phys. Rev. D **93**, 112008 (2016).
- [26] The GERDA Collab., M. Agostini, et al., Nature **544**, **47** (2017).
- [27] The NEMO-3 Collab., R. Arnold et al., Phys. Rev. Lett. **95**, 182302 (2005).
- [28] The NEMO-3 Collab., R. Arnold et al., Phys. Rev. D **92**, 072011 (2015).
- [29] The CAMEO Collab., F.A. Danevich et al., Nucl. Phys. Proc. Suppl. **138**, 230 (2005); The NEMO-3 Collab., R. Arnold et al., Phys. Rev. D **95**, 012007 (2017).
- [30] The CUORE Collab., K. Alfonso et al., Phys. Rev. Lett. **115**, 102502 (2015).
- [31] The KamLAND-Zen Collab., A. Gando et al., Phys. Rev. Lett. **117**, 082503 (2016).
- [32] The NEMO-3 Collab. R. Arnold et al., Phys. Rev. D **94**, 072003 (2016).
- [33] L. D. Landau, Nucl. Phys. **13** 181 (1959).
- [34] R. Eden, D. Landshoff, P. Olive, and J. Polkinhorne, "The analytic S-matrix". International Series In Pure and Applied Physics. McGraw-Hill, New York, 1966.